

## Observation of Enhanced Monopole Strength and Clustering in $^{12}\text{Be}$

Z. H. Yang (杨再宏),<sup>1</sup> Y. L. Ye (叶沿林),<sup>1,\*</sup> Z. H. Li (李智焕),<sup>1</sup> J. L. Lou (楼建玲),<sup>1</sup> J. S. Wang (王建松),<sup>2</sup> D. X. Jiang (江栋兴),<sup>1</sup> Y. C. Ge (葛愉成),<sup>1</sup> Q. T. Li (李奇特),<sup>1</sup> H. Hua (华辉),<sup>1</sup> X. Q. Li (李湘庆),<sup>1</sup> F. R. Xu (许甫荣),<sup>1</sup> J. C. Pei (裴俊琛),<sup>1</sup> R. Qiao (乔锐),<sup>1</sup> H. B. You (游海波),<sup>1</sup> H. Wang (王赫),<sup>1,3</sup> Z. Y. Tian (田正阳),<sup>1</sup> K. A. Li (李阔昂),<sup>1</sup> Y. L. Sun (孙叶磊),<sup>1</sup> H. N. Liu (刘红娜),<sup>1,3</sup> J. Chen (陈洁),<sup>1</sup> J. Wu (吴锦),<sup>1,3</sup> J. Li (李晶),<sup>1</sup> W. Jiang (蒋伟),<sup>1</sup> C. Wen (文超),<sup>1,3</sup> B. Yang (杨彪),<sup>1</sup> Y. Y. Yang (杨彦云),<sup>2</sup> P. Ma (马朋),<sup>2</sup> J. B. Ma (马军兵),<sup>2</sup> S. L. Jin (金仕纶),<sup>2</sup> J. L. Han (韩建龙),<sup>2</sup> and J. Lee (李晔菁)<sup>3</sup>

<sup>1</sup>State Key Laboratory of Nuclear Physics and Technology, School of Physics, Peking University, Beijing 100871, China

<sup>2</sup>Institute of Modern Physics, Chinese Academy of Science, Lanzhou 730000, China

<sup>3</sup>RIKEN Nishina Center, 2-1 Hirosawa, Wako, Saitama 351-0198, Japan

(Received 10 December 2013; published 22 April 2014)

In a recent breakup-reaction experiment using a  $^{12}\text{Be}$  beam at 29 MeV/nucleon, the  $0^+$  band head of the expected  $^4\text{He} + ^8\text{He}$  molecular rotation was clearly identified at about 10.3 MeV, from which a large monopole matrix element of  $7.0 \pm 1.0 \text{ fm}^2$  and a large cluster-decay width were determined for the first time. These findings support the picture of strong clustering in  $^{12}\text{Be}$ , which has been a subject of intense investigations over the past decade. The results were obtained thanks to a specially arranged detection system around zero degrees, which is essential in determining the newly emphasized monopole strengths to signal the cluster formation in a nucleus.

DOI: 10.1103/PhysRevLett.112.162501

PACS numbers: 21.60.Gx, 25.60.Gc, 25.70.Ef, 25.70.Mn

Nucleon clustering inside a nucleus is an intriguing phenomenon which has given rise to an alternative view of the basic structure of a nucleus [1,2] and also generated significant impact on the formation of elements in the universe [3]. The coexistence of mean-field dynamics and clustering dynamics, which are manifested dramatically and alternatively for limited energy changes, is a unique feature of a nuclear many-body system [4].

Recently it has been recognized that, compared to usual  $\alpha$ -conjugate nuclei [5], a much larger number of cluster (molecular) configurations can be formed in an unstable nucleus, owing to numerous combinations of valence nucleons with the cluster cores [4]. Studies on such a new aspect of nuclear clustering have acquired strong interest in recent years [4,6]. However, although remarkable progress has been made from the theoretical side [4,6–8], only a few cluster states have been experimentally justified, focusing mainly on the stable nuclei [9]. Conclusive identification of a cluster state is challenging, since it usually requires experimental determination of the excitation energy ( $E_x$ ) and spin-parity associated with a rotational band, the cluster decay width and, more convincingly, the characteristic transition strength [10].

Neutron-excess Be isotopes are obvious good candidates of clustering studies, for the richness of their cluster structures built on a well-established  $\alpha + \alpha$  rotor of  $^8\text{Be}$  [7], and also the availability of necessary beams from the newly developed radioactive ion beam facilities world wide. In the case of  $^{12}\text{Be}$ , the observation of the  $N = 8$  shell quenching [11] was a signal of  $\alpha$  clustering [9]. In a pioneering work by A. A. Korshennikov *et al.* [12],

hints of cluster decay from an excited state around 10 MeV were found. Soon after, from a breakup reaction of  $^{12}\text{Be}$  at 31.5 MeV/nucleon, Freer *et al.* reported an observation of several resonant states, which form rotational bands with very large moments of inertia [13,14], in accordance with the molecular structure expected theoretically [7,15]. However, some of these resonant peaks, especially those at higher relative energies ( $E_{\text{rel}}$ ), could not be confirmed in a later experiment using a  $^{12}\text{Be}$  beam at a higher incident energy (50 MeV/nucleon) [16]. The authors of Ref. [16] tentatively attributed this inconsistency to the possible larger “background” at higher collision energies. Indeed, the analysis of the reaction mechanism in the framework of antisymmetrized molecular dynamics (AMD) has favored an optimum incident energy range of 20–30 MeV/nucleon for cluster studies via the breakup reaction [17]. We notice that a few other measurements for  $^{12}\text{Be}$  excitation and decays were also reported in the literature [18–20].

From Freer’s experiment, the  $4^+$ ,  $6^+$  and  $8^+$  resonant states in  $^{12}\text{Be}$  were identified in the  $^6\text{He} + ^6\text{He}$  channel, while similar states for the  $^4\text{He} + ^8\text{He}$  channel were also reported with certain ambiguities [13,14]. The nonobservation of the low-lying  $0^+$  and  $2^+$  states in their measurement was owing to the lack of detection around zero degrees, resulting in very low detection efficiency for near-threshold states with small relative energies ( $E_{\text{rel}}$ ). Meanwhile, it has been emphasized in recent studies that the monopole transition, often related to the near-threshold low spin states, is a sensitive probe of the cluster formation in light nuclei [4,21]. So far this probe has rarely been

applied to unstable nuclei, due to the lack of absolute measurements for cross sections of the related resonances.

In this Letter, we report on a new breakup-reaction experiment for  $^{12}\text{Be}$ , in which the detection was concentrated on the most forward angles. The  $0^+$  resonant state in the  $^4\text{He} + ^8\text{He}$  channel was clearly identified, from which an enhanced monopole strength and a large cluster decay width were extracted. These findings demonstrate a typical clustering structure in  $^{12}\text{Be}$ .

The experiment was carried out at the Radioactive Ion Beam Line at the Heavy Ion Research Facility in Lanzhou (HIRFL-RIBLL) [22]. A layout of the detection system can be found in our previous publication [23]. A 29 MeV/nucleon  $^{12}\text{Be}$  secondary beam with an intensity of about  $3 \times 10^3$  particles per second and a purity of about 70% was produced from a  $^{18}\text{O}$  primary beam at 70 MeV/nucleon. Two parallel plate avalanche chambers (PPACs) with position resolutions of about 1 mm (FWHM) in both the  $X$  and  $Y$  directions were employed to track the beam onto a 100 mg/cm $^2$  carbon target. The charged fragments were recorded by a downstream zero-degree telescope consisting of a double-sided silicon strip detector (DSSD) and a  $4 \times 4$  CsI(Tl) scintillator array. The angular coverage of the telescope is about  $0^\circ$ – $12^\circ$ . The DSSD has a thickness of 300  $\mu\text{m}$  and an active area of  $64 \times 64$  mm $^2$  with its front and back faces each divided into 32 strips. Each CsI(Tl) scintillator unit has a size of  $2.5 \times 2.5 \times 3.0$  cm $^3$  and is backed by a photodiode readout. Energy calibrations of the telescope were achieved using a  $^{241}\text{Am}$   $\alpha$ -particle source together with beams of  $^6\text{He}$  and  $^4\text{He}$  produced from the  $^{18}\text{O}$  primary beam. In the present work we are interested in events with two fragments recorded in coincidence. Particle identification (PID) for these multiplicity-2 events, composed of mostly  $^4\text{He}$ ,  $^6\text{He}$ , and  $^8\text{He}$  isotopes, is excellent and was illustrated in Refs. [23,24]. It is worth noting that the accompanying reaction mechanisms, such as  $^{12}\text{C}(^{12}\text{Be}, ^8\text{He})^{16}\text{O}^*$ , can be neglected because our kinematics would correspond to the population and alpha decay of the states in  $^{16}\text{O}$  with excitation energies over 50 MeV.

The  $E_{\text{rel}}$  of a pair of fragments is deduced according to the invariant mass method [25], which has an advantage of being insensitive to the beam energy. The reconstruction performance and the possible contaminations were checked by using the  $^4\text{He} + ^4\text{He}$  coincident events and the empty target counting, respectively [26]. Resonant states in  $^{12}\text{Be}$  obtained from the  $^6\text{He} + ^6\text{He}$  and  $^4\text{He} + ^8\text{He}$  decay channels are presented in Figs. 1(a) and 1(b), respectively, where  $E_x = E_{\text{rel}} + E_{\text{thr}}$  with  $E_{\text{thr}}$  being the decay threshold energy. For comparison, corresponding spectra obtained from Freer's experiment [14] are also plotted in Figs. 1(c) and 1(d), respectively. Monte Carlo simulations were performed to estimate the resolution of  $E_{\text{rel}}$  and the detection efficiency (acceptance) for these  $2^{-X}\text{He}$  events [24,25]. The simulated detection efficiency curve for the

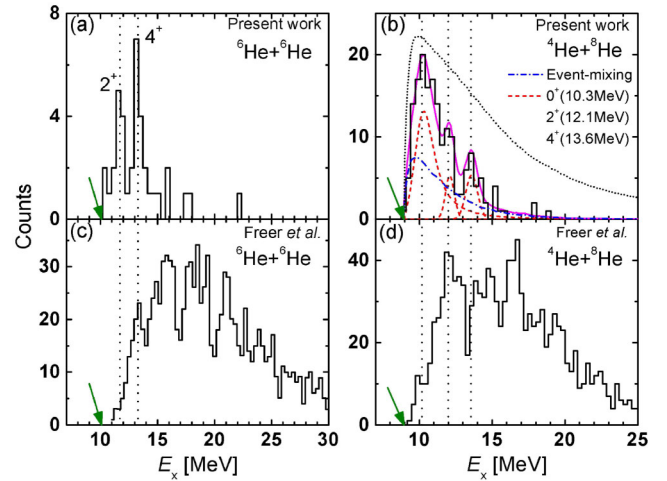


FIG. 1 (color online).  $E_x$  spectra for  $^{12}\text{Be}$ , reconstructed from (a) the  $^6\text{He} + ^6\text{He}$  and (b) the  $^4\text{He} + ^8\text{He}$  coincident fragments, and compared to those reported in Ref. [14], (c) and (d), respectively. The black-dotted curve in (b) displays the simulated detection efficiency (peaking at 49%) of the present experiment. The green arrows indicate the respective cluster decay thresholds. The vertical black-dotted lines are used to guide the peak positions.

$^4\text{He} + ^8\text{He}$  channel is shown in Fig. 1(b), while that for the  $^6\text{He} + ^6\text{He}$  channel behaves similarly and is not shown here. We note that the efficiency curve for Freer's experiment is shifted toward the higher  $E_{\text{rel}}$  side and covers a broader  $E_{\text{rel}}$  range [14].

Since resonances in the  $^6\text{He} + ^6\text{He}$  channel have been analyzed in depth [13], they provide a base to verify the consistency between the present and the previous measurements. In Fig. 1(a), two peaks at 11.7 and 13.3 MeV are well formed, although the number of counts is quite limited. The width (FWHM) of each peak ( $\sim 1$  MeV) is consistent with the experimental resolution ( $\sim 0.8$  MeV) estimated from the simulation [24]. The 13.3 MeV state agrees well with the 13.2 MeV state reported in Ref. [14], which was assigned a spin parity of  $4^+$  based on an angular correlation analysis, and also is consistent with the 13.5 MeV state presented in Ref. [16]. The peak at 11.7 MeV is a new observation of the present experiment, owing to the high detection efficiency at small  $E_{\text{rel}}$ . Following the systematics of the molecular rotational (MR) band proposed in Ref. [13], a spin parity of  $2^+$  might be assigned to this new state. Indeed we have examined the polar angle distributions for the 11.7 and 13.3 MeV peaks in the framework of the distorted-wave Born approximation (DWBA) [27] and the consistency with the  $2^+$  and  $4^+$  assignments, respectively, was indeed found.

Data in the  $^4\text{He} + ^8\text{He}$  channel [Fig. 1(b)] have higher statistics and thus allow a comprehensive analysis. In the spectrum three peaks are seen at about 10.3, 12.1, and 13.6 MeV. The 12.1 MeV peak agrees nicely with that

observed by Freer *et al.* [14]. According to theoretical predictions for the  ${}^4\text{He} + {}^8\text{He}$  MR band [7,9], the spin parities of  $2^+$  and  $4^+$  might tentatively be assigned to the 12.1 and 13.6 MeV states, respectively. We have verified the  $4^+$  assignment using both the angular correlation (refer to Ref. [13] and also the descriptions below) and DWBA analyses. A new and remarkably large peak stands around 10.3 MeV in Fig. 1(b). We note that our detection efficiency around this peak is about 5 times larger than that for Freer's experiment, but both become equal at  $E_x \sim 13.5$  MeV [14,24]. Thus the scaled spectrum shapes in Figs. 1(b) and 1(d) [also Figs. 1(a) and 1(c)] are consistent with each other. As a matter of fact, Charity *et al.*, in Ref. [16], have noticed a "shoulder" around 10.2 MeV for both hydrogen and carbon targets, which well resembles the large peak observed here when scaled by the acceptance. There is also a hint of a wide peak at around 10 MeV in the spectrum measured by Saito *et al.* [19], although beneath it is seen a quite high background. The multipole decomposition analysis [20] has allowed them to extract the excitation-energy spectra for various spin-parity components, including the one for  $0^+$  with a peak close to 10 MeV (see Fig. 2 of Ref. [20]). As indicated in many studies [28], the direct (nonresonant) breakup or phase-space distribution is inevitable for  $E_x$  just above the decay threshold, and thus should be subtracted from the resonant cross section. Such background can be simulated by employing the "event-mixing" technique [29], and its contribution to the present  $E_x$  spectrum is illustrated in Fig. 1(b) (blue dot-dashed line). A function composed of three peaks together with an "event-mixing" term is used to fit the experimental  $E_x$  spectrum. We adopt a Breit-Wigner (BW) shape for the first peak around 10.3 MeV in order to evaluate its formation and decay natures [9]. The BW function is convoluted with the energy response function and filtered by the acceptance [24]. Gaussian functions with widths determined from the

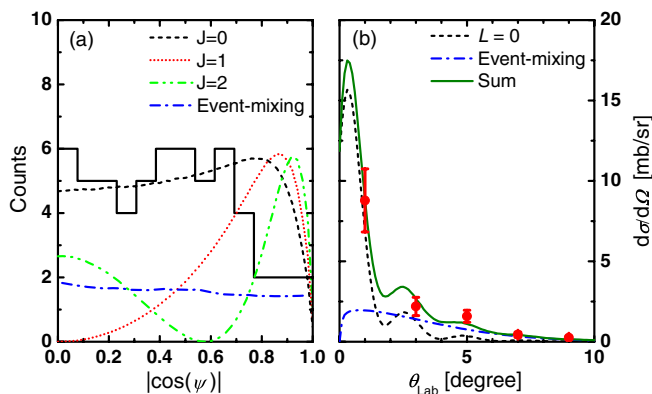


FIG. 2 (color online). (a) Angular correlation distribution as described in the text (calculations are normalized to the data), for inelastic scattering of  ${}^{12}\text{Be}$  at 29 MeV/nucleon from a carbon target, reconstructed from the  ${}^4\text{He} + {}^8\text{He}$  decay channel; (b) differential cross sections compared with DWBA calculations.

detection resolution are used for the other two peaks at higher energies. The best result obtained from a least-square fitting is shown by the magenta solid curve in Fig. 1(b). The extracted (observed) width of the BW function is  $\Gamma = 1.5(2)$  MeV (the error is statistical only).

We applied the model-independent angular correlation method, as described in Ref. [13], to examine the spin of the above 10.3 MeV resonance. For small angle inelastic scattering leading to a resonant state with an angular momentum  $J$ , which subsequently breaks up into spin-0 fragments, the projected angular correlation spectrum is proportional to  $|P_J(\cos(\Psi))|^2$ , with  $\Psi$  being the c.m. angle relative to the beam direction. Owing to the symmetry property of the  $|P_J(\cos(\Psi))|^2$  function and the uniform behavior of the experimental distribution over the whole range of  $\cos(\Psi)$ , the analysis is performed against  $|\cos(\Psi)|$  only, in order to have a better statistical presentation [Fig. 2(a)]. In the calculations the detection efficiency has been taken into account. The loss of events in the data distribution and the drop down of the theoretical curves, at the large-value end of  $|\cos(\Psi)|$ , are due to the ineffectiveness of the coincident measurement for  $2\text{-}^x\text{He}$  fragments which enter into the same CsI(Tl) crystal. The estimated uncertainty in  $|\cos(\Psi)|$  is less than  $\pm 0.1$ , over most of the  $|\cos(\Psi)|$  range. In Fig. 2(a), the experimental data are plotted for spin 0, which are also meaningful for other spins since the defined correction does not affect the spectrum shape owing to the small angle detection [13]. As evidenced in the figure, the spin-0 component is consistent with the data, whereas spin 1 and spin 2 (and higher spins with more oscillations) contradict the experimental distribution [30]. Data in Fig. 2(a) are gated on a  $E_x$  range of 10.0 to 11.4 MeV in order to reduce contamination from the event-mixing component and higher energy peaks [Fig. 1(b)]. The same kind of analyses were also performed for gates at both sides of the 10.3 MeV peak and the results look the same as in Fig. 2(a), indicating a high purity of the spin-0 component in this resonance. As mentioned above such angular correlation analysis was also applied to the 13.6 MeV peak [Fig. 1(b)], and the observed oscillations coincide well with the  $4^+$  expectation, demonstrating a high sensitivity of this method and a good resolution on  $|\cos(\Psi)|$ .

The differential cross section as a function of polar angle (in lab frame) is also built as shown in Fig. 2(b) (filled circles), in which the sharp increase at small angles again characterizes a spin-0 state [31]. A DWBA calculation for inelastic excitation was performed, using optical potentials proposed in Ref. [32]. The theoretical curve is convoluted with the simulated angular resolution and scaled by the angular acceptance [24]. Together with a background term representing the direct breakup process (blue-dotted curve), the calculation, assuming a pure  $0^+$  final state, reproduces well the experimental data (green-solid curve). As pointed out in Refs. [21,33], persistence of a strong monopole

strength comparable to the typical single-particle strength (e.g., a matrix element of  $3.37 \text{ fm}^2$  for the  $0p \rightarrow 1p$  transition [33]) for excited states below 20 MeV signals the formation of cluster structure. This is because, within a simple single-particle picture, the monopole transition would cause a  $2\hbar\omega$  (about 35 MeV) jump, and hence the single-particle monopole strength should vanish for lower-lying states [21]. Well-established examples of enhanced monopole strengths associated with cluster formation include those from the  $0_1^+$  ground state to the  $0_2^+$  (7.65 MeV) state in  $^{12}\text{C}$ , and to the  $0_2^+$  (6.05 MeV) and  $0_3^+$  (12.05 MeV) states in  $^{16}\text{O}$  [34]. Very recently, Ito *et al.* have implemented the generalized two-center model (GTCM), based on an assumption of preformed molecular configurations [7]. Extensive calculations were performed for  $^{12}\text{Be}$ , in which four  $0^+$  resonant states were predicted, lying in an  $E_x$  range of 9 to 20 MeV [7]. Amongst them, the  $0_3^+$  state has a dominating  $^4\text{He} + ^8\text{He}$  cluster structure and possesses the largest monopole strength [33]. Now from the differential cross sections [Fig. 2(b)] measured from the  $^4\text{He} + ^8\text{He}$  decay channel, we are able to extract the respective part of this strength, which may be regarded as its lowest limit. A normalization factor of 0.034(10) was applied to the DWBA calculation to fit the data [Fig. 2(b)]. This factor is multiplied by 2.2 to account for the fraction of events belonging to the  $0^+$  peak but outside the applied energy gate (10.0–11.4 MeV). The energy-weighted sum rule (EWSR) for all monopole transitions in  $^{12}\text{Be}$  is  $6727.9 \text{ fm}^4 \text{ MeV}$ , deduced according to  $\frac{2\hbar^2}{m} AR_{\text{rms}}^2$  [35], with  $m$  the nucleon mass,  $A = 12$  and  $R_{\text{rms}} = 2.59(6) \text{ fm}$  [36]. Thus the monopole matrix element is deduced [21,35] to be  $7.0 \pm 1.0 \text{ fm}^2$ , comparable to the typical enhanced ones in  $^{12}\text{C}$  and  $^{16}\text{O}$  as denoted above [34] and consistent with the cluster part of strength predicted in Ref. [33]. Additionally a systematic error of about 12% should be considered for this matrix element, taking into account the uncertainties in the DWBA and EWSR calculations, the energy and spatial resolutions of the detection system, and the shapes of the  $0^+$  peak and event-mixing components in Fig. 1(b).

The energy-spin systematics of the  $^4\text{He} + ^8\text{He}$  and  $^6\text{He} + ^6\text{He}$  rotational bands are plotted in Fig. 3 (right panel). The GTCM calculations reproduce well the experimental data for the  $^4\text{He} + ^8\text{He}$  channel. The GTCM approach, which is formulated on a basis of molecular structure, also provides a consistent calculation of the resonant cross section (the left panel in Fig. 3)[9], in which the  $^4\text{He} + ^8\text{He}$  band head has a width as large as the total width [ $\Gamma = 1.5(2) \text{ MeV}$ ] determined from the present experiment. The AMD approach also suggested a particularly large width for a cluster band head just above the threshold [37]. However, the determination of the cluster partial width needs further quantitative evaluation. According to the energy thresholds and phase spaces of all decay channels of  $^{12}\text{Be}$  [26], the 10.3 MeV state decays

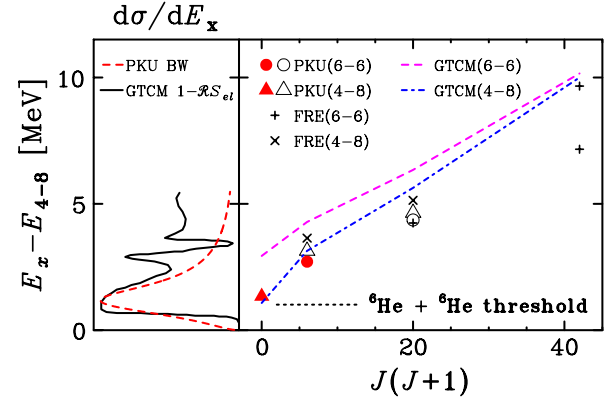


FIG. 3 (color online). Energy-spin systematics for resonant states in  $^{12}\text{Be}$  (right panel).  $E_{4-8}$  (reference energy of the vertical axis) is the separation energy of the  $^4\text{He} + ^8\text{He}$  channel. The black short-dashed line at the bottom indicates the decay threshold for the  $^6\text{He} + ^6\text{He}$  channel. The curves in the left panel are the partial reaction cross sections for the  $0^+$  strength.

predominantly either to the binary helium clusters ( $^4\text{He} + ^8\text{He}$  and  $^6\text{He} + ^6\text{He}$ ) with a partial width  $\Gamma_{\text{He}}$ , or to the  $^{10-12}\text{Be}$  isotopes via neutron or  $\gamma$  ( $e^+e^-$  pair) emissions with a partial width  $\Gamma_{\text{Be}}$ , possessing  $\Gamma = \Gamma_{\text{He}} + \Gamma_{\text{Be}}$  [9,38]. In Ref. [12], Koshennilov *et al.* have reported an excited state at about 10 MeV in  $^{12}\text{Be}$ , which decays to  $^{10-12}\text{Be}$  isotopes with  $\Gamma/\Gamma_{\text{Be}} = 3.6 \pm 1.6$ . Such a state was populated from a general inelastic excitation process. Since, in the c.m. frame, the dominance of a monopole-excitation cross section at small angles should averagely persist at larger angles (see, e.g., Fig. 1 of Ref. [39]), the resonances (or “shoulders”) around 10 MeV reported in Refs. [12,14,16] and from our present work, do match with each other. Thus it is reasonable to infer that the cluster branching ratio  $\Gamma_{\text{He}}/\Gamma = 1 - \Gamma_{\text{Be}}/\Gamma = 0.72(12)$  and the cluster partial width  $\Gamma_{\text{He}} = 1.1(2) \text{ MeV}$  for the presently observed 10.3 MeV state. In addition, since within the  $E_x$  range of this  $0^+$  state, the number of the observed  $^6\text{He} + ^6\text{He}$  events is negligible compared to the  $^4\text{He} + ^8\text{He}$  events [see Figs. 1(a) and 1(b)], even correcting for the respective efficiency curves,  $\Gamma_{\text{He}}$  here is indeed dominated by the  $^4\text{He} + ^8\text{He}$  configuration. Using  $\Gamma_{\text{He}}$ , we can further obtain a reduced decay width  $\gamma_{\text{He}}^2 = 0.50(9) \text{ MeV}$  and a dimensionless reduced width  $\theta_{\text{He}}^2 = 0.53(10)$ , based on a standard  $R$ -matrix analysis [38] in which a channel radius  $R = 1.4 \times (8^{1/3} + 4^{1/3}) = 5.0 \text{ fm}$  is adopted [37]. The large  $\Gamma_{\text{He}}/\Gamma$  and  $\theta_{\text{He}}^2$  demonstrate a high level of clustering in the 10.3 MeV ( $0^+$ ) state in  $^{12}\text{Be}$  [38].

In summary, a new breakup-reaction experiment for  $^{12}\text{Be}$  at 29 MeV/nucleon was carried out. For the first time a remarkably large peak around 10.3 MeV with a spin parity of  $0^+$  is identified in  $^{12}\text{Be}$ , leading to an enhanced monopole matrix element of  $7.0 \pm 1.0 \text{ fm}^2$  in the  $^4\text{He} + ^8\text{He}$  decay channel. This resonant state possesses a large cluster-decay branching ratio, corresponding to a large

dimensionless reduced width of 0.53(10). These results reveal a typical clustering structure in  $^{12}\text{Be}$ , in agreement with the GTCM prediction. Other resonances observed in both  $^4\text{He} + ^8\text{He}$  and  $^6\text{He} + ^6\text{He}$  decay channels are complementary to the previously suggested MR bands. The application of a zero degree telescope was essential in our experiment which focused on the detection of the near-threshold resonances. It would be desirable to further apply this technique to investigate the strong monopole transition related to cluster formation in unstable nuclei.

We thank the staffs of HIRFL-RIBLL for their technical and operation support. The valuable discussions with M. Ito, M. Freer, Y. H. Zhang, and X. H. Zhou are gratefully acknowledged. This work has been supported by the 973 program of China (No. 2013CB834402) and NSFC Projects (No. 11035001, No. 11275011, No. 11235001, No. J1103206).

---

\*Corresponding author.  
yeyl@pku.edu.cn

- [1] L. R. Hafstad and E. Teller, *Phys. Rev.* **54**, 681 (1938).
- [2] M. G. Mayer, J. H. D. Jensen, *Elementary Theory of Nuclear Shell Structure* (Wiley, New York, 1955).
- [3] F. Hoyle, *Astrophys. J.* **1**, 12 (1954).
- [4] H. Horiuchi, K. Ikeda, and K. Kat, *Prog. Theor. Phys. Suppl.* **192**, 1 (2012).
- [5] K. Ikeda, N. Tagikawa, H. Horiuchi, *Prog. Theor. Phys. Suppl.* **E68**, 464 (1968).
- [6] W. von Oertzen, M. Freer, and Y. Kanada-En'yo, *Phys. Rep.* **432**, 43 (2006).
- [7] M. Ito, N. Itagaki, H. Sakurai, and K. Ikeda, *Phys. Rev. Lett.* **100**, 182502 (2008).
- [8] B. Zhou, Y. Funaki, H. Horiuchi, Z. Ren, G. Röpke, P. Schuck, A. Tohsaki, C. Xu, and T. Yamada, *Phys. Rev. Lett.* **110**, 262501 (2013).
- [9] M. Ito, *Phys. Rev. C* **85**, 044308 (2012).
- [10] W. N. Catford, *J. Phys. Conf. Ser.* **436**, 012085 (2013).
- [11] S. D. Pain *et al.*, *Phys. Rev. Lett.* **96**, 032502 (2006).
- [12] A. A. Korshennikov *et al.*, *Phys. Lett. B* **343**, 53 (1995).
- [13] M. Freer *et al.*, *Phys. Rev. Lett.* **82**, 1383 (1999).
- [14] M. Freer *et al.*, *Phys. Rev. C* **63**, 034301 (2001).
- [15] M. Dufour, P. Descouvemont, and F. Nowacki, *Nucl. Phys.* **A836**, 242 (2010).
- [16] R. J. Charity *et al.*, *Phys. Rev. C* **76**, 064313 (2007).
- [17] H. Takemoto, H. Horiuchi, and A. Ono, *Phys. Rev. C* **63**, 034615 (2001).
- [18] N. Curtis *et al.*, *Phys. Rev. C* **73**, 057301 (2006).
- [19] A. Saito *et al.*, *Nucl. Phys.* **A738**, 337 (2004).
- [20] A. Saito *et al.*, *Mod. Phys. Lett. A* **25**, 1858 (2010).
- [21] T. Yamada, Y. Funaki, T. Myo, H. Horiuchi, K. Ikeda, G. Röpke, P. Schuck, and A. Tohsaki, *Phys. Rev. C* **85**, 034315 (2012).
- [22] Z. Sun, W.-L. Zhan, Z.-Y. Guo, G. Xiao, and J.-X. Li, *Nucl. Instrum. Methods Phys. Res., Sect. A* **503**, 496 (2003).
- [23] H. B. You *et al.*, *Nucl. Instrum. Methods Phys. Res., Sect. A* **728**, 47 (2013).
- [24] Z. H. Yang, and Y. L. Ye, *Eur. Phys. J. Web of Conferences* **66**, 02112 (2014).
- [25] Z. X. Cao *et al.*, *Phys. Lett. B* **707**, 46 (2012).
- [26] N. I. Ashwood *et al.*, *Phys. Lett. B* **580**, 129 (2004).
- [27] I. J. Thompson, *Comput. Phys. Rep.* **7**, 167 (1988).
- [28] A. Spyrou *et al.*, *Phys. Rev. Lett.* **108**, 102501 (2012); **109**, 239202 (2012).
- [29] M. Assie *et al.*, *Eur. Phys. J. A* **42**, 441 (2009).
- [30] M. Freer *et al.*, *Phys. Rev. Lett.* **96**, 042501 (2006).
- [31] D. H. Youngblood, Y.-W. Lui, and H. L. Clark, *Phys. Rev. C* **55**, 2811 (1997).
- [32] M. Buenerd, *Nucl. Phys.* **A424**, 313 (1984).
- [33] M. Ito, *Phys. Rev. C* **83**, 044319 (2011).
- [34] T. Yamada, Y. Funaki, H. Horiuchi, K. Ikeda, Y. Funaki, and A. Tohsaki, *Prog. Theor. Phys.* **120**, 1139 (2008).
- [35] G. R. Satchler and D. T. Khoa, *Phys. Rev. C* **55**, 285 (1997).
- [36] A. Ozawa, T. Suzuki, and I. Tanihata, *Nucl. Phys.* **A693**, 32 (2001).
- [37] Y. Kanada-En'yo, and H. Horiuchi, *Phys. Rev. C* **68**, 014319 (2003).
- [38] M. Alcorta *et al.*, *Phys. Rev. C* **86**, 064306 (2012).
- [39] G. R. Satchler, *Nucl. Phys.* **A472**, 215 (1987).